ISSN 1063-7834, Physics of the Solid State, 2018, Vol. 60, No. 3, pp. 532–536. © Pleiades Publishing, Ltd., 2018.
Original Russian Text © T.V. Drokina, G.A. Petrakovskii, M.S. Molokeev, D.A. Velikanov, 2018, published in Fizika Tverdogo Tela, 2018, Vol. 60, No. 3, pp. 526–530.

FERROELECTRICITY

Synthesis, Crystal Structure, and Magnetic Properties of the $YbFeTi_2O_7$ Compound

T. V. Drokina[a, *], G. A. Petrakovskii[a], M. S. Molokeev[a, b, c], and D. A. Velikanov[a]

[a] *Kirensky Institute of Physics, Federal Research Center KSC, Siberian Branch, Russian Academy of Sciences, Krasnoyarsk, 660036 Russia*

[b] *Far Eastern State Transport University, Khabarovsk, 680000 Russia*

[c] *Siberian Federal University, Krasnoyarsk, 660041 Russia*

**e-mail: tvd@iph.krasn.ru*

Received June 28, 2017

Abstract—We report on the synthesis conductions and results of experimental investigations of the crystal structure and magnetic properties of a new magnetic compound $YbFeTi_2O_7$. According to the X-ray diffractometry data, the crystal structure of the investigated compound is described by the rhombic space group *Pcnb* with unit cell parameters of $a = 9.8115(1)$ Å, $b = 13.5106(2)$ Å, and $c = 7.31302(9)$ Å and atomic disordering in the distribution of iron ions Fe^{3+} over five structural sites. The magnetic measurements in the low-temperature region revealed a kink in the temperature dependence of the magnetic moment and its dependence on the sample magnetic prehistory. The experimental results obtained suggest that with a decrease in temperature the sample passes from the paramagnetic state to the spin-glass-like magnetic state characterized by a freezing temperature of $T_f = 4.5$ K at the preferred antiferromagnetic exchange coupling in the sample spin system. The chemical pressure variation upon replacement of rare-earth ion R by Yb in the $RFeTi_2O_7$ system does not change the crystal lattice symmetry and magnetic state.

DOI: 10.1134/S1063783418030095

1. INTRODUCTION

Due to the keen interest in the search for new materials promising for application in various fields of engineering and chemical industry, synthesis of substances with different magnetic properties and magnetic ordering types has still been an urgent problem of physics of condensed matter. In view of this, of great importance are the development and fabrication of magnetic materials, including oxide compounds containing rare-earth magnetic ions and transition metal ions, which are characterized by the competition of magnetic interactions.

As is known, new magnetic compounds with the general formula $RFeTi_2O_7$ (the rare-earth ion R^{3+} = Sm, Gd, Dy, Tu, Tb, or Lu), the crystal symmetry of which is described by the rhombic space group *Pcnb*, are characterized by the atomic disordering of the distribution of magnetic iron ions over different structural sites and exhibit the magnetic spin-glass-like state [1–5]. It is interesting to study the variation in the chemical composition of the $RFeTi_2O_7$ system and structural and magnetic properties of the samples with the cation substitution, which changes the chemical pressure.

In this study, we report on the results of synthesis and investigations of the properties of a new magnetic material $YbFeTi_2O_7$. X-ray diffractometry and magnetic measurement data are presented.

2. EXPERIMENTAL

The $YbFeTi_2O_7$ compound was synthesized by the solid-state reaction from the mixture of Fe_2O_3 (25.2 mass %), Yb_2O_3 (62.2 mass %), and TiO_2 (12.6 mass %) oxides. The tableted samples with a diameter of 10 mm and a thickness of 1.5–2.0 mm were annealed at temperatures of 1200–1250°C under normal pressure. The synthesis procedure included four annealings with the intermediate wet milling in alcohol and repeated pressing stages. The chemical and phase composition of the synthesized samples was controlled by X-ray diffraction (XRD) analysis.

The $YbFeTi_2O_7$powder XRD patterns was obtained on a Bruker D8 Advance diffractometer (CuK_α radiation) using a Vantec linear detector. The experiment was carried out using a varying scan rate (VSR) and varying scan step (VSS) technique. The time of exposure increased with the angle 2θ, which significantly improved the quality of recorded XRD patterns [6–8]. As a rule, the full width at half maximum (FWHM) of the peak should contain 5–8 experimental points. However, the peaks significantly broaden with

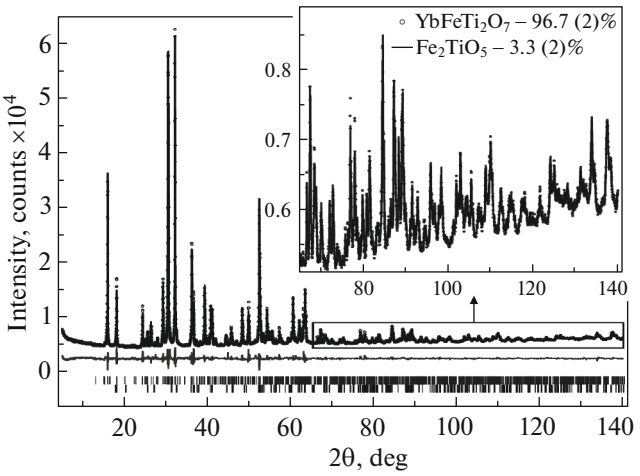

Fig. 1. XRD pattern of the polycrystalline $YbFeTi_2O_7$ compound at room temperature. Difference XRD pattern (lower curve). The investigated substance contains 5.87% of Fe_2TiO_5 impurity.

increasing 2θ angle. Therefore, we increased a step in the regions of the large 2θ angle to reduce the experimental time [9]. Then, the experimental data were converted in one *XYE* file conventionally used in X-ray diffractometery, which contains the coordinates $2\theta_i$, intensity I_i, and standard deviation $\sigma(I_i)$ for each experimental point. The Rietveld refinement implemented, e.g., in the TOPAS 4.2 program [10] takes into account a standard deviation of each point via calculating its weight $w_i = 1/\sigma(I_i)^2$. Thus, the increase in the exposure time for a point leads to a decrease in the standard deviation $\sigma(I_i)$ and, consequently, to the larger weight w_i in the least-squares refinement. In the VCT technique, the weights of weak high-angle and strong low-angle reflections are equated, whereas in the conventional experiment the weights are unequal, so the information on the structure contained in the high-angle region is lost.

The experimental XRD pattern of the investigated $YbFeTi_2O_7$ sample was obtained using the VCT/VSS technique and divided into four parts: 5–38.7°C (exposure at point 3 s, the step is 0.016°), 38.7–61.6°C (exposure at point 9 s, the step is 0.024°), 61.6–97.5°C (exposure at point 15 s, the step is 0.032°), and 97.5–140°C (exposure at point 24 s, the step is 0.040°). The total experimental time was 16 h. The experiment was divided in parts using the XRD Wizard program [9]. The peak positions were determined using the EVA (2004 release) program from the Bruker DIFFRAC-PLUS package.

The experiments on determination of the temperature behavior of the magnetic moment were carried out on an MPMS-XL magnetometer (Siberian Federal University) in the temperature range of 2–300 K in a magnetic field of 500 Oe.

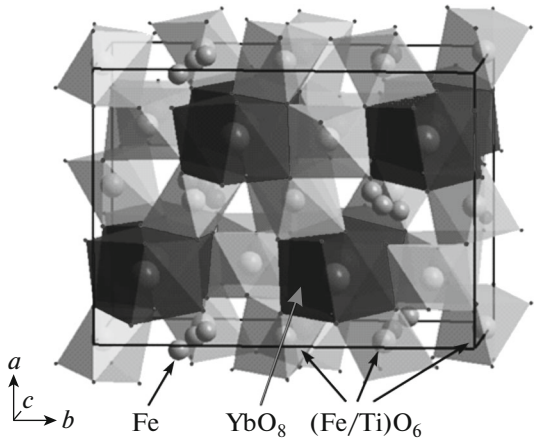

Fig. 2. Crystal structure of the $YbFeTi_2O_7$ compound.

3. EXPERIMENTAL RESULTS

The structural properties of the polycrystalline $YbFeTi_2O_7$ compound were studied by XRD analysis (see the XRD pattern in Fig. 1). The XRD data on the synthesized sample show that it contains, along with the ground $YbFeTi_2O_7$ phase, a minor Fe_2TiO_5 impurity (3.3(2)%).

Since the investigated compound is isostructural to $GdGaTi_2O_7$ [11], we took the $GdGaTi_2O_7$ structure as an initial model of the $YbFeTi_2O_7$ crystal structure. According to the XRD data obtained, the $YbFeTi_2O_7$ crystal symmetry at room temperature is described by the rhombic space group *Pcnb*. It is worth noting that the Yb^{3+} ion has the smallest ionic radius (R = 1.00 Å [12]) among rare-earth magnetic ions. Comparison with other $RFeTi_2O_7$ well-known compounds [1–5] showed that the chemical pressure variation under cation substitution R → Yb, as well as Sm, Gd, Dy, Tu, Tb, and Lu, does not change the crystal lattice symmetry of zirconolites.

The main crystallographic characteristics and experimental parameters for the $YbFeTi_2O_7$ compound are given in Table 1. The atomic coordinates and refined atomic site occupancies p in the $YbFeTi_2O_7$ material are given in Table 2. Figure 2 shows the $YbFeTi_2O_7$ compound crystal structure. It follows from Table 2 that the $YbFeTi_2O_7$ crystal structure contains five nonequivalent iron ion positions and three of them are mixed (Fe/Ti). This facilitates their random population by Fe^{3+} ions.

The unit cell of the crystal lattice of the investigated compound contains $0.94 \times 8 + 0.59 \times 4 + 0.77 \times 8 =$ 16 Ti atoms and $0.06 \times 8 + 0.41 \times 4 + 0.23 \times 8 + (0.78 \times 4 + 0.11 \times 8) = 8$ Fe atoms. Thus, taking into account the relative occupancies of individual sites, the resulting formula can be written as $YbFe_{1.00(5)}Ti_{2.00(5)}O_7$.

Table 1. Main crystallographic characteristics of $YbFeTi_2O_7$ and X-ray diffraction experiment parameters

Space group	*Pcnb*
a, Å	9.8115(1)
b, Å	13.5106(2)
c, Å	7.31302(9)
V, Å^3	969.41(2)
Z	8
D_x, g/cm^3	5.963
μ, mm^{-1}	84.016
2θ interval, deg	5–140
Number of reflections	927
Number of refined parameters	74
R_{wp}, %	1.911
R_{exp}, %	0.671
R_p, %	1.751
GOF (χ^2)	2.850

Titanium ions in the multiatomic $YbFeTi_2O_7$ crystal are in the diamagnetic state Ti^{4+}. The magnetic subsystem of the investigated compound is formed by ions of two types: rare-earth ytterbium ions Yb^{3+} (electron configuration $4f^{14}6s^2$) and iron ions Fe^{3+} (electron configuration $3d^5$). Figures 3 and 4 present the results of magnetic measurements of the $YbFeTi_2O_7$ compound.

The temperature dependence of the inverse magnetic susceptibility $\chi^{-1}(T)$ of the $YbFeTi_2O_7$ sample cooled in a field of $H = 500$ Oe in the temperature range of 2–300 K is shown in Fig. 3. Analysis of the temperature dependence of the inverse magnetic susceptibility $\chi^{-1}(T)$ in the high-temperature region $T >$ 100 K showed that this dependence is described by the Curie–Weiss law. In the high-temperature region, the sample is in the paramagnetic state characterized by the negative asymptotic Neel temperature $\theta = -127$ K, which is indicative of the predominance of antiferromagnetic interaction in the complex magnetic subsystem of the sample under study with *d* and *f* elements. Table 3 gives experimental asymptotic Neel temperatures θ, Curie–Weiss constants *C*, and calculated and experimental effective moments in the temperature range where the magnetic susceptibility obeys the Curie–Weiss law. The calculated effective magnetic moment of the $YbFeTi_2O_7$ formula unit is $\mu_{eff\,cal} = 7.48\mu_B$ ($\mu_{eff\,cal}^{Fe^{3+}} = 5.91\mu_B$ and $\mu_{eff\,cal}^{Yb^{3+}} = 4.59\mu_B$). The Curie–Weiss constant is $C = 0.016$ K, which corresponds to the effective magnetic moment (molar value) $\mu_{eff\,exp} = 4.58\mu_B$. The experimental effective magnetic moment is comparable with the numerically calculated value.

The magnetic measurements (see the data in Fig. 4) showed that below the temperature $T_f = 4.5$ K, the temperature dependence of the magnetic moment $M(T)$ of the $YbFeTi_2O_7$ sample depends on its prehistory, i.e., on whether it was cooled in a magnetic field of $H = 0.05$ T or without it. Thus, the observed $M(T)$ dependences show that at low temperatures ($T < T_f =$

Table 2. Atomic coordinates, site occupancies *p*, and heat parameters B_{iso} of the $YbFeTi_2O_7$ compound

Atom	Position multiplicity	*x*	*y*	*z*	*p*	B_{iso}, Å^2
Yb	8	0.2459(3)	0.13233(12)	0.0040(5)	1	0.57(8)
Ti1	8	0.2454(11)	0.3847(4)	0.4867(12)	0.94(2)	0.5(1)
Fe1	8	0.2454(11)	0.3847(4)	0.4867(12)	0.06(2)	0.5(1)
Ti2	4	0.5	0.25	0.248(3)	0.59(5)	0.5(2)
Fe2	4	0.5	0.25	0.248(3)	0.41(5)	0.5(2)
Ti3	8	0.0060(8)	0.4858(4)	0.2548(17)	0.77(3)	0.9(2)
Fe3	8	0.0060(8)	0.4858(4)	0.2548(17)	0.23(3)	0.9(2)
Fe	4	0	0.25	0.327(2)	0.78	0.7(2)
Fei	8	0.025(6)	0.278(4)	0.175(9)	0.11	0.7(2)
O1	8	0.1624(9)	0.3909(11)	0.248(6)	1	1.0(2)
O2	8	0.4027(19)	0.1112(15)	0.252(6)	1	1.0(2)
O3	8	0.109(2)	0.1509(10)	0.245(5)	1	1.0(2)
O4	8	0.366(4)	0.277(3)	0.449(5)	1	1.0(2)
O5	8	0.370(4)	0.280(3)	0.060(5)	1	1.0(2)
O6	8	0.374(3)	0.494(2)	0.427(4)	1	1.0(2)
O7	8	0.381(3)	0.483(2)	0.050(4)	1	1.0(2)

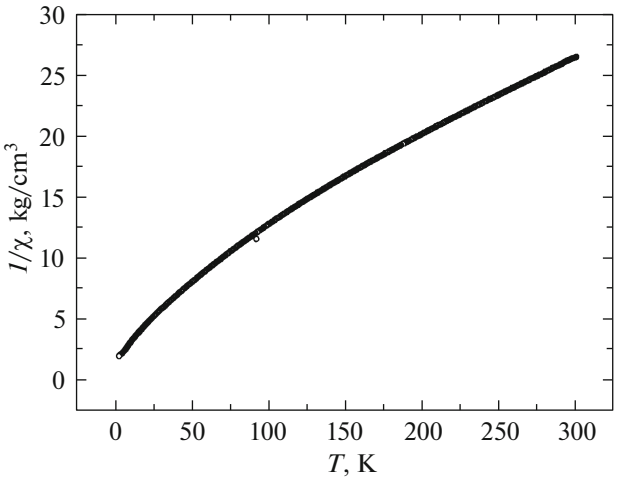

Fig. 3. Temperature dependence of the inverse magnetic susceptibility of the $YbFeTi_2O_7$ sample cooled in a field of $H = 0.05$ T. The sample mass is $m = 0.045$ g. The asymptotic Neel temperature is $\theta = -127$ K.

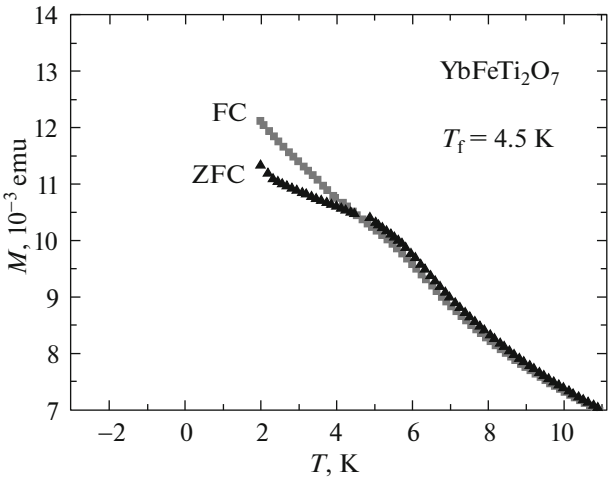

Fig. 4. Low-temperature dependence of the $YbFeTi_2O_7$ magnetic moment obtained in two measurement modes: cooling in a magnetic field of $H = 0.05$ T (FC) and zero field cooling (ZFC). The measurements were performed in a magnetic field of $H = 0.05$ T. The sample mass is $m = 0.045$ g. The freezing temperature is $T_f = 4.5$ K.

4.5 K), there are several magnetic moment values, depending on the sample cooling conditions. It should be noted that the magnetic measurement data obtained in the low-temperature region are typical of the samples with the spin-glass-like magnetic state. The atomic disordering in the iron distribution over the crystal lattice and randomly changed interactions between magnetic atoms apparently lead to the formation of the spin-glass-like magnetic state at temperatures below a freezing temperature of $T_f = 4.5$ K.

The obtained experimental data characterizing the magnetic properties of the investigated compound are consistent with the results of experiments conducted on different samples upon replacement of the rare-earth cation R^{3+} in the $RFeTi_2O_7$ system, where R = Sm, Gd, Dy, Tu, Tb, or Lu [1–5].

Based on the above-described features of the distribution of iron ions over the crystal lattice, magnetic measurement data, and comparison with the properties of other $RFeTi_2O_7$ (R = Sm, Gd, Dy, Tu, Tb, or Lu) compounds, we may assume that in the $YbFeTi_2O_7$ sample at temperatures below $T_f = 4.5$ K, the frozen spatial distribution of orientations of the spin magnetic moments forms due to the presence of randomly distributed magnetic moments and competing interactions in the system, as well as the magnetic moment frustration, which is apparently caused by them. Note that the estimation of the frustration level ($F = |\theta|/T_f$ [13]) yielded its high value (28.2).

Thus, both the crystal lattice symmetry and the magnetic state in the $RFeTi_2O_7$ (R = Yb, Sm, Gd, Dy, Tu, Tb, or Lu) system are independent of the ionic radius of the rare-earth ion. The formation of magnetic properties of the $YbFeTi_2O_7$ compound representing the family of compounds with the general formula $RFeTi_2O_7$ is caused by the complex interplay of competing exchange couplings between the neighboring magnetic atoms.

Table 3. Asymptotic Neel temperatures θ, Curie–Weiss constants C, and calculated and experimental effective moments of the $YbFeTi_2O_7$ compound

Compound	$YbFeTi_2O_7$
Freezing temperature T_f, K	4.5
Asymptotic Neel temperature θ, K	−127
Curie–Weiss constant C, K	0.016
$\mu_{eff\,cal} = (\mu_1^2 + \mu_2^2)^{1/2}$, where $\mu_i = g_i[J_i(J_i+1)]^{1/2}$, μ_B	7.49
$\mu_{eff\,exp}$, μ_B	7.48

4. CONCLUSIONS

Using the solid-state synthesis, we obtained a new magnetic compound $YbFeTi_2O_7$.

We established the crystal lattice and proved the existence of nonequivalent crystallographic sites of the high-spin cation Fe^{3+} and the presence of atomic disorder in the distribution over the $YbFeTi_2O_7$ crystal lattice at room temperature. Taking into account the relative occupancies of individual positions, we can write the crystallochemical formula of the investigated compound as $Yb^{3+}Fe^{3+}_{1.00(5)}Ti^{4+}_{2.00(5)}O^{2-}_7$.

Study of the magnetic properties in the temperature range of 2–300 K showed that the paramagnetic state at temperatures above 100 K obeys the Curie–Weiss law and is characterized by the negative asymptotic Neel temperature, which is indicative of the predominance of the antiferromagnetic exchange coupling in the spin system of the $YbFeTi_2O_7$ compound. In the low-temperature region, the sample magnetization depends not only on temperature, but also on the cooling conditions (FC or ZFC). Based on the set of experimental data and comparison with the properties of other previously investigated compounds from the $RFeTi_2O_7$ (R = Sm, Gd, Dy, Tu, Tb, or Lu) series, we assumed that the $YbFeTi_2O_7$ magnet has the spin-glass-like state with a freezing temperature of $T_f = 4.5$ K.

In addition, the experimental data showed that the chemical pressure variation by means of the cation substitution of R^{3+} in the $RFeTi_2O_7$ system does not change the crystal structure symmetry or, apparently, the magnetic state.

The newly synthesized magnetic material broadens the class of compounds with the high frustration level and requires further investigations.

REFERENCES

1. G. A. Petrakovskii, T. V. Drokina, A. L. Shadrina, D. A. Velikanov, O. A. Bayukov, M. S. Molokeev, A. V. Kartashev, and G. N. Stepanov, Phys. Solid State **53**, 1855 (2011).
2. G. A. Petrakovskii, T. V. Drokina, D. A. Velikanov, O. A. Bayukov, M. S. Molokeev, A. V. Kartashev, A. L. Shadrina, and A. A. Mitsuk, Phys. Solid State **54**, 1813 (2012).
3. T. Drokina, G. Petrakovskii, M. Molokeev, A. Arauzo, and J. Bartolome, Phys. Proc. **12**, 580 (2015).
4. T. Drokina, G. Petrakovskii, D. Velikanov, and M. Molokeev, Solid State Phenom. **215**, 470 (2014).
5. T. V. Drokina, G. A. Petrakovskii, M. S. Molokeev, D. A. Velikanov, O. N. Pletnev, and O. A. Bayukov, Phys. Solid State **55**, 2037 (2013).
6. I. C. Madsen and R. J. Hill, Adv. X-ray Anal. **35**, 39 (1992).
7. I. C. Madsen and R. J. Hill, J. Appl. Cryst. **27**, 385 (1994).
8. W. I. F. David, Abstract P2.6, NIST Spec. Publ. No. 846 (NIST, Gaithersburg, 1992), p. 210.
9. *Diffrac-Plus Basic XRD Wizard* (Bruker AXS, Karlsruhe, Germany, 2002–2007).
10. Bruker AXS, *TOPAS V4: General Profile and Structure Analysis Software for Powder Diffraction Data, User's Manual* (Bruker AXS, Karlsruhe, Germany, 2008).
11. E. A. Genkina, V. I. Andrianov, E. L. Belokoneva, B. V. Mill', B. A. Maksimov, and R. A. Tamazyan, Sov. Phys. Crystallogr. **36**, 796 (1991).
12. K. P. Belov, M. A. Belyanchikova, R. Z. Levitin, and S. A. Nikitin, *Rare Earth Ferro and Antiferromagnetics* (Nauka, Moscow, 1965) [in Russian].
13. J. A. Mydosh, *Spin-Glasses: An Experimental Introduction* (Taylor, New York, 1993).

Translated by E. Bondareva